

TASK: TW5-TTMI-004
IFMIF, Design Integration

Deliverables: a) Deuteron-induced activation cross-section evaluation for the Fe isotopes by means of optical model potential analysis and b) Deuteron-induced activation cross-section evaluation for accelerator materials (Cu, Al, Nb and others but excluding the already studied corrosion products of the Li-target)

M. Avrigeanu, V. Avrigeanu, and F.L. Roman

“Horia Hulubei” National Institute of R&D for Physics and Nuclear Engineering, Magurele

1. Introduction

A compilation of the elastic scattering data for deuterons on the stable isotopes of Al, Cu and Nb, for D-energies up to 50 MeV, proves the existence of angular distributions for deuterons on ^{27}Al at only 14 energies between 5 and 58.7 MeV, on $^{63,65,\text{nat}}\text{Cu}$ at 9 energies between 11.8 and 34.4 MeV, and ^{93}Nb at 4 energies between 11.8 and 52 MeV, and two values of total reaction cross section of deuterons on each ^{27}Al and $^{\text{nat},63,65}\text{Cu}$ between 11 and 25 MeV. However, the description of deuteron-nucleus interaction represents an important test for both the quality of semi-microscopic optical models and evaluation of nuclear data requested for fusion reactor technology, while the difficulties to interpret the data in terms of the usual optical-model potential (OMP) hampered such a comprehensive analysis. The weak binding of the deuteron results in significant contributions of the breakup channel and enhances a variety of reactions at low bombarding energy. Nevertheless, a semi-microscopic analysis appears as the most suitable basis for the evaluation of the deuteron-induced activation cross sections necessary for fusion applications.

On the other hand, while the full phenomenological OMP [1] led to a good description of the $d+^6,7\text{Li}$ data, proving its reliability at variance with the use of extrapolation of the older deuteron global potentials over a wider range of mass and energy domains, the semi-microscopic optical potential [2] has record some questions concerning the microscopic real optical potential component as well as the spin-orbit one. Therefore, the semi-microscopic analysis of deuteron elastic scattering on ^6Li at low incident energy was considered firstly as an useful way for setting up the method of deuteron-induced activation calculation for accelerator materials (Al, Fe, Cu, Nb) in the last three months of 2005 and also in the whole 2006.

2. Semi-microscopic analysis of deuteron elastic scattering at low incident energy

This work is based on previous IFIN-HH studies of the realistic effective nucleon-nucleon (NN) interactions by using the double-folding (DF) model for the semi-microscopic optical potential [3,4]. The calculated microscopic real potential have been obtained by using the M3Y, BDM3Y, and DDM3Y Paris effective NN interactions,

and a sensitivity analysis of calculated cross sections with respect to effective NN interactions is planned in order to establish the proper use of DF nuclear potential for complex particles [1,3,5] including deuterons. The elastic scattering of deuterons has been calculated for energies up to 50 MeV by using a modified version of the OMP computer code SCAT2 [6] (NEA Data Bank). The interaction potential has included a Coulomb term, the DF real potential and an imaginary part of global parameter sets by Daehnick *et al* [7], Lohr and Haerberli [8] or Perey and Perey [9].

The deuteron density distribution has been obtained from the *s*-state wave function calculated with both Paris and CD-Bonn [10] potentials, and from the experimental charge form factors measured by Abbot *et al.* [11]. Since the two *s*-state wave functions are very close, the corresponding density distributions lead to essentially identical folded potentials. Therefore, in the present analysis we have chosen the Abbot deuteron density distribution for the DF potential calculation. The first step of the semi-microscopic analysis of the deuteron interaction with Li isotopes was dedicated to the spin-orbit component of the semi-microscopic optical potential. Firstly, the microscopic Watanabe [12] spin-orbit potential was included in the semi-microscopic optical potential, leading to no significant improvement of experimental data description. Thus, the spin-orbit potential obtained by the phenomenological analysis of deuteron scattering on $^{6,7}\text{Li}$, with constant depth and geometry, is included in the present OMP.

The second step of the analysis was dedicated to the nonlocality correction to the microscopic real potential, in order to obtain an equivalent local DF potential:

$$U_{\text{DF}}^{\text{EELP}}(r) \approx U_{\text{DF}}(r) + c_{\text{non}} d^2 U_{\text{DF}}(r)/dr, \quad (1)$$

Where the empirical nonlocality parameter c_{non} has been obtained from the fit of experimental elastic-scattering differential cross sections. The semi-microscopic angular distributions obtained with this Empirical Equivalent Local double-folded Potential (EELP) compared with the experimental ones (Figure 1) show now an improved description of the angular distributions, mainly at forward and backward angles for low and, respectively, higher incident energies.

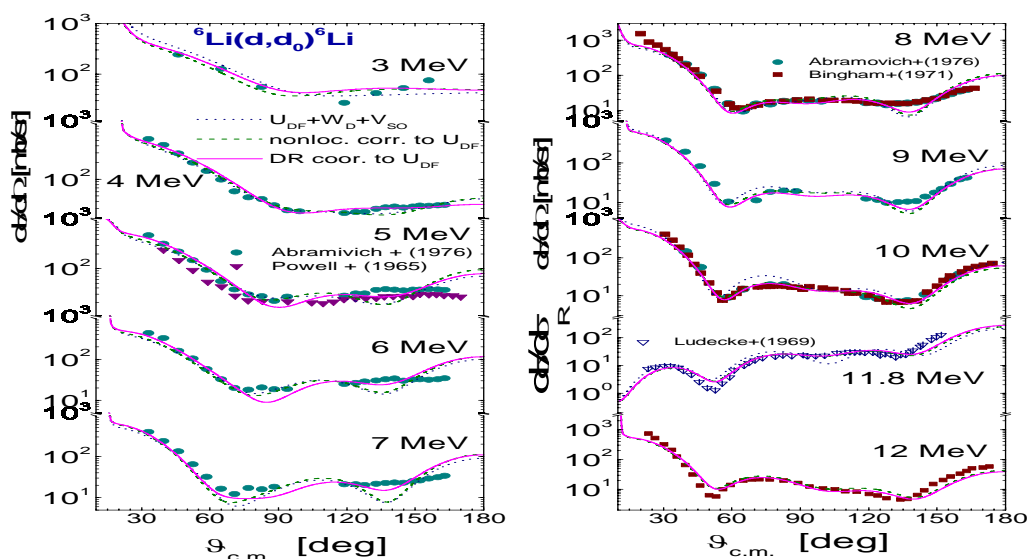


Figure 1. Comparison of experimental and semi-microscopic elastic-scattering differential cross sections of deuterons interacting with ^6Li between 3 and 12 MeV, obtained with the DF potential (dotted curve), EELP potential (dashed curve), as well as the EELP potential with dispersion correction (solid curve).

Finally, the dispersion correction [13] has been added to the EELP, based on the energy dependence of the imaginary potential. As an overall conclusion, a better description of the experimental data has been obtained for all angular distributions analyzed. On the other hand, it has been tried to find a convenient nonlocality correction easy to be incorporated in the practical calculations performed with semi-microscopic potentials. The improved description of the elastic differential cross sections obtained with the empirical equivalent local potential stressed both the proper change of the semi-microscopic potential and the corresponding sensitivity of the calculated cross sections.

3. Average energy-dependent phenomenological OMP for the system $d+^{27}\text{Al}$

3.1 Semi-microscopic optical potential

The deuteron elastic-scattering experiments also on ^{27}Al at incident energies lower than 20 MeV are not satisfactory described by any of the phenomenological global OMPs of either Daehnick et al. [7], Lohr-Haeberli [8], or Perey-Perey [9] (Figure 2). Moreover, results from analysis of the low-energy elastic scattering data suffer from discrete and continuous ambiguities in the OMP parameters, whose uncertainties vary for various target nuclei and for different incident energies due to the precision of data analyzed. Thus, in order to avoid too much phenomenology in these data description, the phenomenological real potential of Woods-Saxon (WS) type is replaced by the DFM microscopic potential while phenomenological parameters corresponding to imaginary and spin-orbit terms are obtained by fit of the experimental double-differential cross sections. It should be emphasized that for the real part no adjustable parameter or normalization constant was involved in this analysis in order to couple the imaginary and spin-orbit part of the OMP so that the predictive power of this semi-microscopic potential is preserved. As a first result, this approach may reduce the number of the OMP parameters and corresponding uncertainties.

Therefore we have looked for imaginary and spin-orbit potential parameters able to describe the whole body of elastic-scattering double differential cross sections for ^{27}Al from 5 up to 63 MeV. Comparison of the experimental elastic-scattering angular distributions of deuterons on ^{27}Al from 5 to 63 MeV with OMP calculations based on the DF approach obtained by using the M3Y-Paris effective NN interactions, and the deuteron density distribution obtained from the experimental charge form factors [11] (solid curves) as well as by using the predictions given by the global OMP of Daehnick et al. [7] (dot-dashed curves) and Lohr-Haeberli [8] (dashed curves) respectively is shown in Figure 3.

3.2 Phenomenological optical potential

The second step of the present analysis has concerned the determination of an OMP real part by keeping fixed the imaginary and spin-orbit potential parameters obtained within the semi-microscopic analysis, in order to obtain the full phenomenological OMP needed for application calculations. The advantage of having well settled already at least half of the usual OMP parameters increases obviously the accuracy of fitting the data. The calculated elastic scattering cross sections from 5 to 63 MeV by using the real, imaginary and spin-orbit potential parameters obtained by fit of the experimental data at various incident energies are shown in Figure 4 (a, b).

Finally, based on the corresponding local OMP parameters, average energy dependent OMP parameters have been obtained and the corresponding angular distributions are shown in Figure 4 (a-b) by solid curves. Thus, an improved description of the experimental data from 5 to 63 MeV is proved with respect to the predictions of Daehnick et al. [7], Lohr-Haeberli [8], and Perey-Perey [9] global OMPs, which can be considered a suitable validation of the actual potential.

The only couple of measured reaction cross sections are shown in Figure 4(c) in comparison with the calculated values by using the present average OMP for $d+^{27}\text{Al}$, the global Daehnick et al. [7] OMP (dot-dashed curve), as well as the evaluated data of the library ACSELAM [14] (dotted curve).

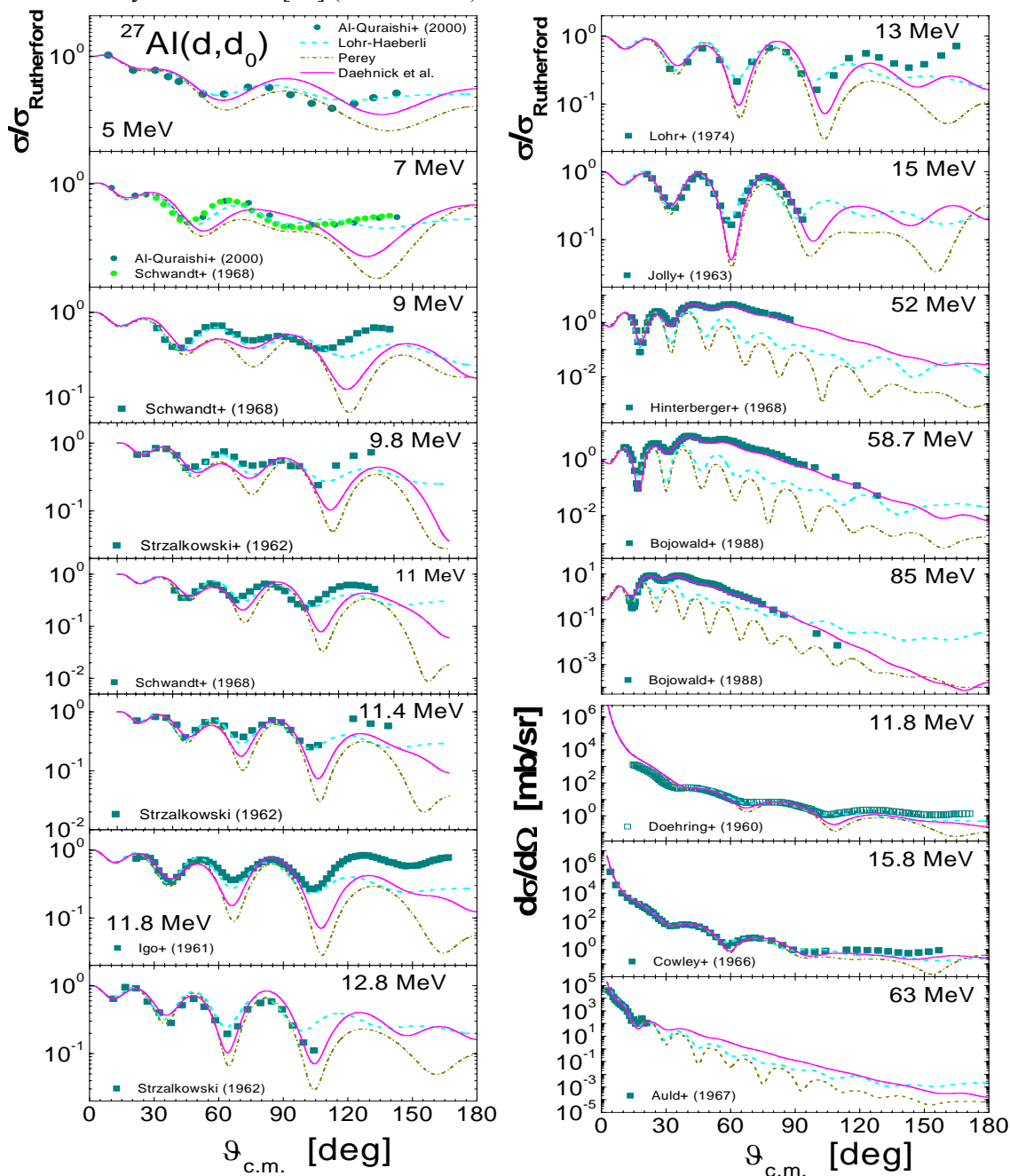


Figure 2. Comparison of the experimental and calculated differential cross sections of the elastic scattering of deuterons on ^{27}Al between 5 and 63 MeV, by using the global parameter sets of Daehnick et al. [7] (solid curves), Lohr-Haeberli [8] (dashed curves) and Perey and Perey [9] (dot-dashed curves).

4. Calculation of deuteron activation cross-sections of ^{27}Al up to 50 MeV

The final goal of this work concerned the calculation of the deuteron-induced activation cross-section calculation for ^{27}Al which has been carried out by using (i) the deuteron average energy-dependent phenomenological OMP following the above-mentioned semi-microscopic analysis,

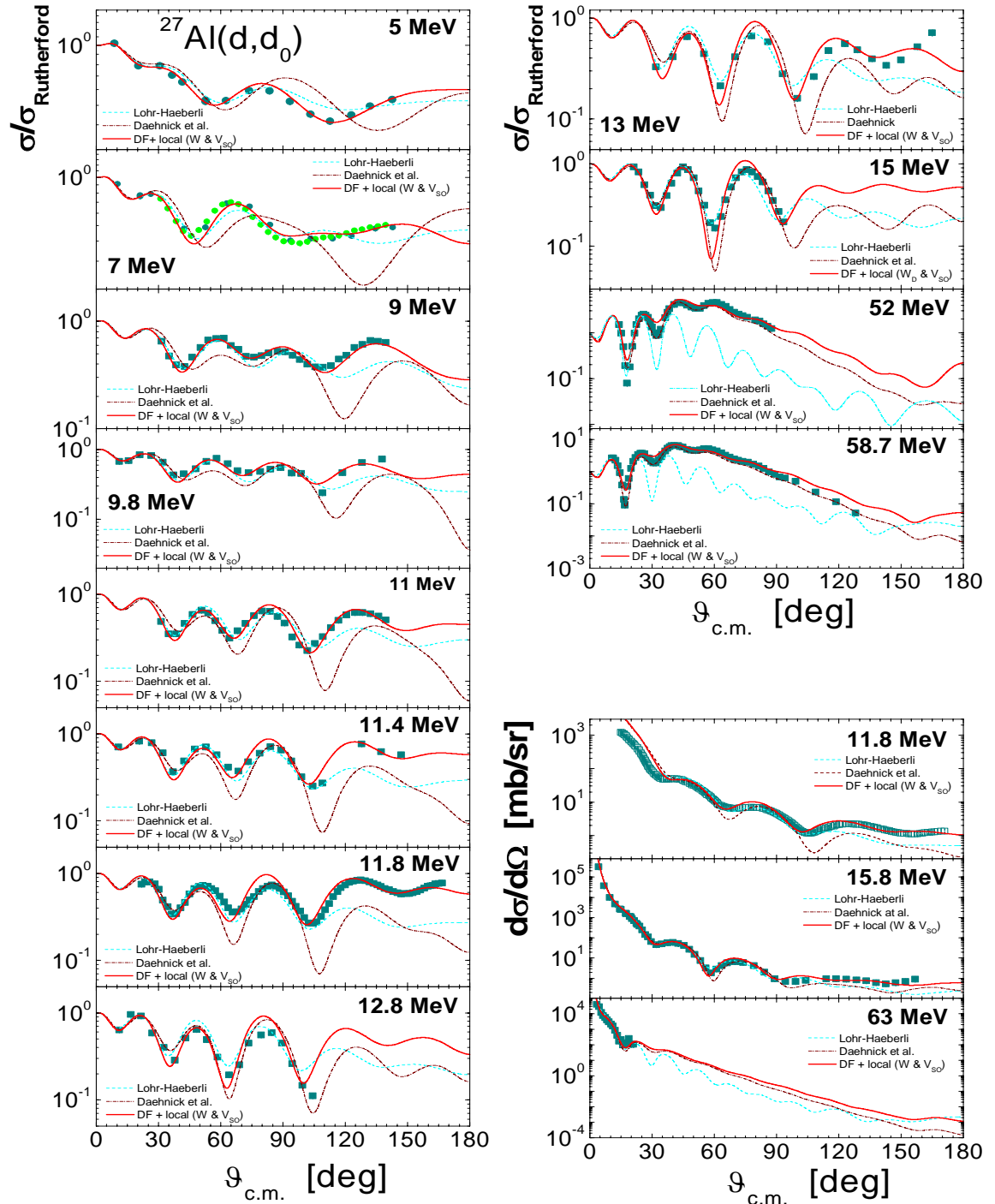


Figure 3. Comparison of the experimental and calculated elastic-scattering differential cross sections of the deuterons on ^{27}Al between 5 and 63 MeV by using the semi-microscopic OMP (solid curves), as well as global parameter sets of Lohr-Haeberli [8] (dashed curves) and Daehnick et al. [7] (dot-dashed curves).

involved within (ii) the direct reaction, pre-equilibrium emission (PE) and Hauser-Feshbach (HF) statistical-model computer codes TALYS [15] and EMPIRE-II [16]. These calculations were done by using the corresponding global input parameter sets excepting the deuteron OMP.

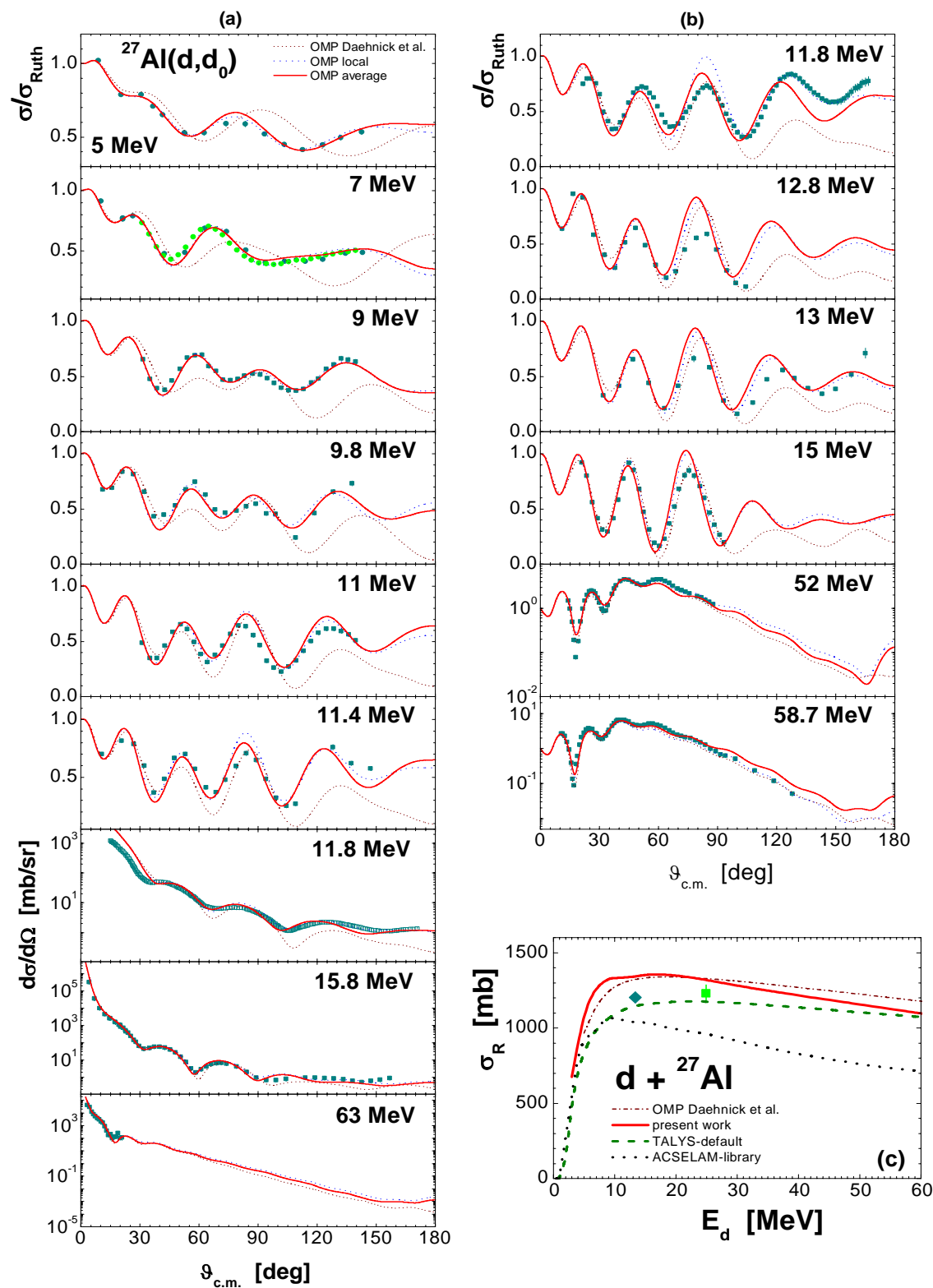


Figure 4. (a-b) Comparison of the experimental and calculated angular distributions of the elastic scattering of deuterons on ^{27}Al between 5 and 63 MeV, by using the present phenomenological local (dashed curves) and average (solid curves) as well as Daehnick et al. [7] OMP parameters; (c) comparison between the experimental and calculated reaction cross sections for $d + ^{27}\text{Al}$.

On the other hand, we have also compared the results thus obtained with those provided by the default OMP of TALYS and EMPIRE-II codes, i.e. a simplification of folding approach of Watanabe [12] and the nucleon OMP of Koning and Delaroche [17], for the former, and Perey and Perey [9] for the latter. Other useful comparisons for the effects of various deuteron OMP have followed the taking into account of the widely used deuteron parameter sets of Daehnick *et al.* [7] and Lohr and Haerberli [8]. At the same time, the results shown by notation TALYS-0.64+ in Figure 5 have been obtained by means of the keyword 'spherical' in order to enforce a spherical OMP calculation, leading to the treatment of the direct inelastic scattering by the Distorted-Wave Born Approximation (DWBA) method, while the default option is the opposite one. We have used also particularly within these calculations a changed keyword 'sysreaction' with respect to the default option, as the authors [18] are recommending for a high-quality OMP for complex particles (otherwise the reaction cross section for deuterons as complex particles would be taken from systematics of non-elastic cross sections based on empirical expressions). It is of similar importance for the case of deuteron-induced reactions that the last EMPIRE-II version 2.19 offers the advantage of using the exciton PE model also for the cluster emission.

Firstly, one may note the rather identical non-elastic cross sections of deuterons provided by the both TALYS and EMPIRE-II codes as well as by SCAT2 within the OMP analyses described within the sections 3 and 4, which proves also the correctness of using the present OMP within the two computer codes. The difference between using the default and particular options for the keywords 'spherical' and 'sysreaction' in TALYS calculations is shown in Figure 5, for the non-elastic cross section of deuterons incident on ^{27}Al . It is rather equal to the variation due to the change of the present deuteron OMP although in the opposite direction at 60 MeV, but more than twice below 20 MeV. Unfortunately, the status of only few and older experimental data, as well as generally for the $^{27}\text{Al}(d,p)^{28}\text{Al}$ and $^{27}\text{Al}(d,p\alpha)^{24}\text{Na}$ reactions (Figure 5) makes not possible a model validation on their basis.

5. Conclusions

The angular distributions of the elastic-scattered deuterons on $^{6,7}\text{Li}$, and ^{27}Al target nuclei have been analyzed by using also the double-folding model for the microscopic optical potential calculation, and lastly energy-dependent OPMs up to 50 MeV have been obtained. Next, the comparison between the elastic angular distributions calculated with the deuteron global potentials and those obtained from the present OMPs proved the latter as most reliable. Finally, these OMPs have been involved in calculations of activation cross-section of deuterons incident on ^{27}Al , performed by using the well-known computer codes TALYS and EMPIRE-II by replacing their default OMP options for deuterons. Comparison of the corresponding results as well as with those following the use of earlier widely-used global OMP parameter sets is finally proved able to support the calculated activation cross sections in this work, in spite of the actual scarce data basis. The TALYS-0.64 output files of the calculated cross sections shown in Figure 5 are part of this report.

One of the authors (M.A.) acknowledges the hospitality of the Atominstut (AI) der Osterreichischen Universitaeten, Technische Universitaet Wien (TUW) during a staff-mobility visit at the Association EURATOM/OAW in the period 2005.10.02-2005.11.25, for working

together with Prof. Helmut Leeb on the research topic “*Microscopic optical potentials for deuteron interaction with accelerator materials*”. The results of this co-operation are shown in the Section 2 of this report, and they may represent the basis for a project for enhancing mutual co-operations between Associations 2006 entitled “*Optical Potentials for Light Ions*” in the framework of the envisaged EFDA-project at AI/TUW on covariance determination for ^{16}O .

6. Forecast progress for the next year (2006)

Calculation of deuteron-induced activation cross sections for $^{63,65}\text{Cu}$, $^{54,56,57,58}\text{Fe}$, and ^{93}Nb target nuclei up to 50 MeV will be carried out within the EFDA task TW6-TTMI-004 as the deliverables No. 5-6 by using the same nuclear reaction models and analysis method as for the ^{27}Al , in a consistent and unitary way in order to overcome the actual rather scarce data basis.

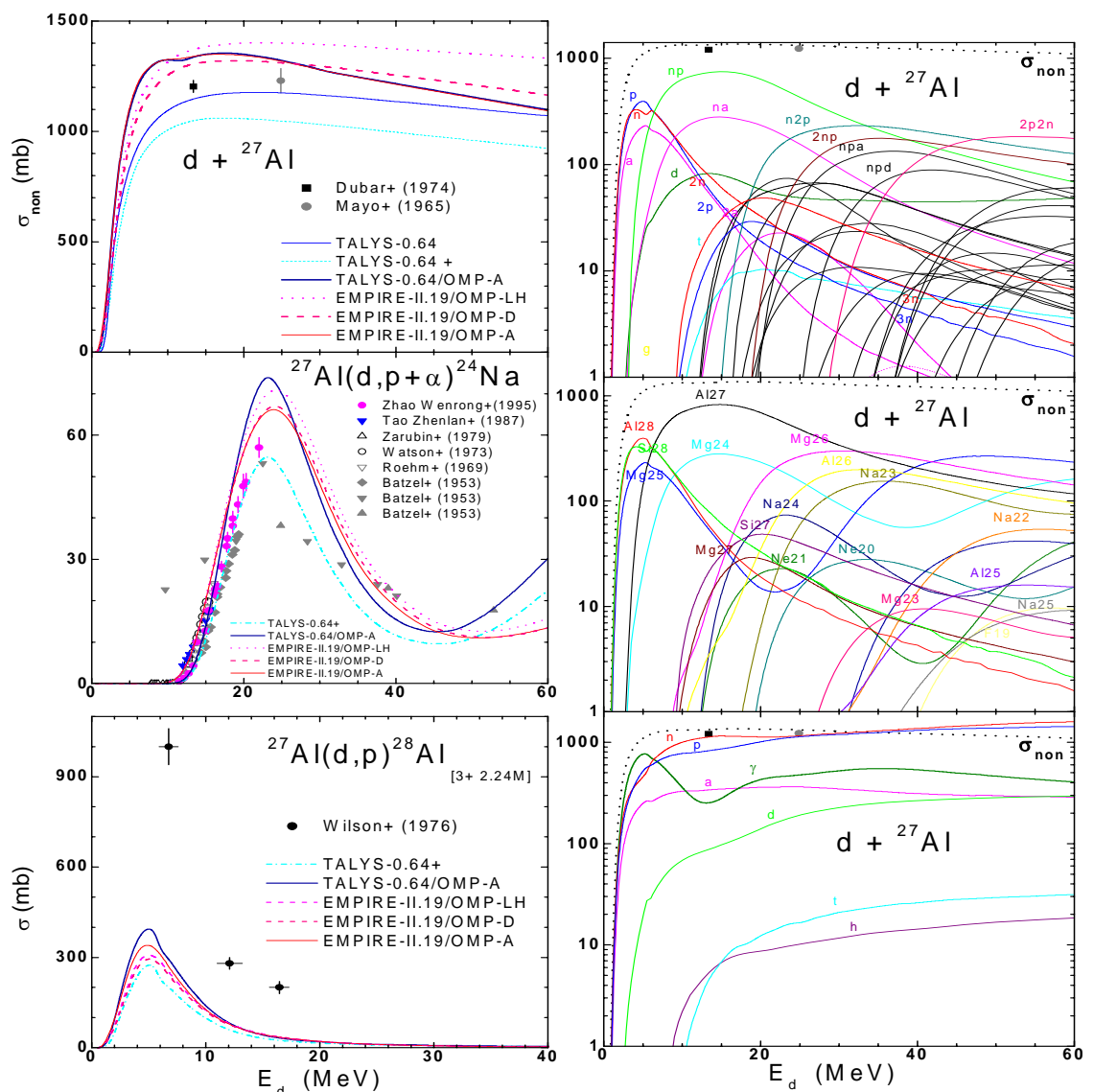


Figure 5. (Left) Comparison of the experimental and calculated non-elastic cross sections (top) as well as (d,p) and (d,p) reaction cross sections for the ^{27}Al target nucleus, by using the TALYS and EMPIRE-II codes with default input parameters excepting the deuteron optical potential either developed in this work (OMP-A) or by Daehnick et al. [7] (OMP-D) and Lohr and Haeberli [8] (OMP-LH). (Right) Various reaction cross sections induced by deuterons on ^{27}Al (top), residual nuclei production (middle), and total particle production cross sections (bottom) obtained by using the code TALYS and the potential OMP-A.

References

- [1] **Avrighianu M., von Oertzen W., Fischer U., Avrighianu V.**, “Analysis of deuteron elastic scattering on ${}^6,7\text{Li}$ up to 50 MeV”, Nucl. Phys. A759 (2005) 327.
- [2] **Avrighianu M., von Oertzen W., Fischer U., and Avrighianu V.**, “Analysis of Deuterium scattering on ${}^6,7\text{Li}$ up to 50 MeV based on realistic effective NN interaction”, in *Nuclear Data for Science and Technology*, R.C. Haight, M.B. Chadwick, T. Kawano, and P. Talou (Eds.), AIP Conf. Proc. No. 769 (2005) 99.
- [3] **Avrighianu M., Anagnostatos G.S., Antonov A.N., Giapitzakis J.**, “On dynamics of two-neutron transfer reactions with the Borromean nucleus ${}^6\text{He}$ ”, Phys. Rev.C 62 (2000) 017001.
- [4] **Avrighianu M., Antonov A.N., Lenske H., Stetcu I.**, “Effective interactions for multistep processes”, Nucl. Phys. A693 (2001) 616.
- [5] **Avrighianu M., von Oertzen W., Plompen A.J.M., Avrighianu V.**, “Optical model potentials for α -particles scattering around the Coulomb barrier on A~100 nuclei”, Nucl. Phys. A723 (2003) 104.
- [6] **Bersillon O.**, Centre d'Etudes de Bruyeres-le-Chatel, Note CEA-N-2227, 1992.
- [7] **Daehnick W.W., Childs J.D., Vrcelj Z.**, Phys. Rev. C 21 (1980) 2253.
- [8] **Lohr J.M., Haeberli W.**, Nucl. Phys. A232 (1974) 381.
- [9] **Perey C.M., Perey F.G.**, Phys. Rev. 132 (1963) 755.
- [10] **Machleidt R.**, Adv. Nucl. Phys. 19 (1989) 189; Phys. Rev. C 63 (2001) 024001.
- [11] **Abbott D., Ahmidouch A., Anklin H., Arvieux J.** et. al., Phys. Rev. Lett. 84 (2000) 5053.
- [12] **Watanabe S.**, Nucl. Phys. 8 (1958) 484.
- [13] **Mahaux C., Ngo H., Satchler G.R.**, Nucl. Phys. A449 (1986) 354; Nucl.Phys. A456 (1986) 134.
- [14] **Tanaka S.** et al., “Development of IRAC code system to calculate induced radioactivity produced by ions and neutrons”, in *Proc. 8th Int. Conf. on Radiation Shielding*, Arlington, April 1994, ANS Inc (1994), vol. 2, p. 965; <http://wwwndc.tokai.jaeri.go.jp/ftpnd/sae/acl.html> .
- [15] **Koning A.J.**, in *Nuclear Model Parameter Testing for Nuclear Data Evaluation*, M. Herman (Ed.), Report INDC(NDS)-431, IAEA, Vienna, 2002, p. 117.
- [16] **Herman M., Oblozinsky P., Capote R., Sin M., Trkov A., Ventura A., Zerkin V.**, in: R.C. Haight, M.B. Chadwick, T. Kawano and P. Talou (Eds.), *Proc. Int. Conf. on Nuclear*

Data for Science and Technology (ND2004), 26 Sept. - 1 Oct. 2004, Santa Fe, New Mexico (AIP, New York, 2005), p. 1184.

[17] **Koning A.J., Delaroche J.P.**, Nucl. Phys. A713 (2003) 231.

[18] **Koning A.J., Hilaire S., Duijvestijn M.C.**, “*TALYS: A nuclear reaction program*”, Report 21297/04.62741/P FAI/AK/AK, NRG-Petten, 2004, p. 40.